

Supplemental Material:

Methods

Mouse models

Cardiac-specific homozygous *atg7* knockout mice (*atg7* cKO) were generated by crossing *Atg7* flox homozygous (fl/fl) mice¹ with α MHC-Cre mice. Cardiac-specific Mito-Keima transgenic mice (Tg-Mito-Keima) were generated using the α MHC promoter. Transgenic mice expressing GFP-LC3 (Tg-GFP-LC3) and cardiac-specific mRFP-GFP-LC3 transgenic mice (Tf-LC3)² have been described. Parkin knock out mice (Parkin KO) and Mitotimer mice were purchased from Jackson Laboratory (Stock No: 006582, and Stock No: 028715). Both sexes of mice were randomly assigned for experimental groups. All experiments were performed with randomization, allocation concealment and blind fashion. All experiments involving animals were approved by the Rutgers-New Jersey Medical School's Institutional Animal Care and Use Committee.

Treatment of mice with either HFD or ND

C57BL/6J wild-type mice, Tg-Mito-Keima, Tg-GFP-LC3, Tf-LC3, *atg7* cKO, and Parkin KO were fed ad libitum with HFD (Research Diets D12492) for 3-12 weeks. A control group of mice matched for age and gender were fed with control diet for the same period of time. Changes in body weight during ND and HFD consumption are shown in **Online Figure XII**. We excluded mice that did not gain 20% of body weight with 2 months' HFD consumption from the subsequent analysis. There were no exclusions among mice fed a ND.

Adult cardiomyocyte (CM) isolation

The method of adult CM isolation has been described³. Mice were anesthetized, and the chest was opened to expose the heart. The descending aorta was cut, and the heart was immediately flushed by injection of 10 mL EDTA buffer into the right ventricle. The ascending aorta was clamped using Reynolds forceps, and the heart was transferred to a 60-mm dish containing fresh EDTA buffer.

Digestion was achieved by sequential injection of 10 mL EDTA buffer, 3mL perfusion buffer, and 30 to 50 mL collagenase buffer into the left ventricle (LV). Constituent chambers (atria, LV, and right ventricle) were then separated and gently pulled into 1-mm pieces using forceps. Cellular dissociation was completed by gentle trituration, and enzyme activity was inhibited by addition of 5 mL stop buffer.

The cell suspension was passed through a 100- μ m filter, and cells underwent 3 sequential rounds of gravity settling, using 3 intermediate calcium reintroduction buffers to gradually restore calcium concentration to physiological levels. The cell pellet in each round was enriched with myocytes and ultimately formed a highly pure myocyte fraction. CM yields and the percentage of viable rod-shaped cells were quantified using a hemocytometer. Then, CMs were resuspended in prewarmed plating media and plated onto laminin precoated plates or coverslips.

Keima with mitochondrial localization signal (Mito-Keima)

Mito-Keima is a mitochondrially localized pH-indicator protein⁴. The method used to detect lysosomal delivery of Mito-Keima has been described⁵.

Flow cytometry

For TMRE (Tetramethylrhodamine ethyl ester, perchlorate) quantification, adult CMs were incubated in media containing 250 nM TMRE at 37°C for 10 min. Cells were analyzed using LSR II flow cytometers (BD Biosciences). All flow cytometry experiments included at least three biological replicates per experiment and were repeated at least three times.

Oil red O staining

Oil red O staining was conducted as described previously⁶. Cryosections of heart tissue samples were used for Oil Red O staining. After fixation in formalin, cardiac tissue slides were incubated with Oil Red O working solution for 15 min, rinsed with 60% isopropanol, rinsed with distilled water for half an hour, then mounted with glycerine jelly.

Triglyceride measurement

Heart samples were homogenized in buffer containing 2 mM NaCl/20 mM EDTA/50 mM sodium phosphate buffer, pH 7.4. Then 10 µl of homogenate was mixed with 10 µl of tert-butyl alcohol and 5 µl of Triton X-100/methyl alcohol mixture (1:1 v/v) for the extraction of lipids. Triglycerides were measured with an Abcam diagnostic kit.

Fatty acid oxidation assay

Fatty acid oxidation was measured by the method described by Watanabe⁷. Isolated adult CMs were incubated with the assay medium in 0.2 ml of 150 mM potassium chloride, 10 mM HEPES, pH 7.2, 0.1 mM EDTA, 1 mM potassium phosphate buffer, pH 7.2, 5 mM Tris malonate, 10 mM magnesium chloride, 1 mM carnitine, 0.15% bovine serum albumin, 5 mM ATP, and 50 µM each fatty

acid (5.0×10^4 cpm of radioactive substrate) for 10 min. The reaction was stopped by the addition of 0.2 ml of 0.6 N perchloric acid and the mixture was centrifuged. Four hundred μ l supernatant, including radioactive degradation products in the water phase was added to 4 ml Scintillation cocktail (Sigma-Aldrich) and radioactivity was measured using a scintillation counter.

Oxygen Consumption assay

A Seahorse XF96 Extracellular Lux Analyzer (Seahorse Bioscience) was used to measure the rate of oxidative phosphorylation in adult CMs⁸.

Tat-Beclin1 (TB1)

The retro-inverso TB1 D-amino acid sequence was RRRQRRKKRGYGGTGFEGDHWIEFTANFVNT⁹. The control peptide, Tat-scramble (TS), consisted of the Tat protein transduction domain, a GG linker, and a scrambled version of the C-terminal 18 amino acids of TB1 (RRRQRRKKRGYGGWETAFGTTEHIFFDNGV). For *in vivo* experiments⁸, D-amino acid peptides were dissolved in H₂O and stored at -80°C until use. For induction of autophagy *in vivo*, mice were injected intraperitoneally with TS or TB1 at 20 mg/kg daily for 2 weeks, beginning 10 weeks after initiation of the HFD.

Evaluation of autophagic flux

To evaluate autophagic flux *in vivo*, chloroquine (CQ) was injected (10mg/kg) intraperitoneally¹⁰. Four hours later, mice were euthanized for immunoblot detection of autophagy markers in the heart.

Electron microscopy (EM)

Conventional EM was performed as described previously¹¹. Lipid droplets were analyzed using Image J.

Real-time qPCR for mitochondrial DNA

Total DNA was extracted from mouse hearts using the DNeasy Blood & Tissue kit (QIAGEN). The mtDNA and nuclear DNA contents were quantified by real-time qPCR of cytochrome b and β -actin respectively as described⁵.

Immunoblot analysis

The methods used for preparation of cell lysates from *in vivo* samples and for immunoblot analyses have been described previously¹². The antibodies used include LC3 (BML,M186-3), Cox IV (CST,4844S), GAPDH (CST,2118S), α -tubulin (Sigma,T9026), Caspase-3 (CST, 9662S) and Cleaved Caspase-3 (CST,9661S), Parkin (CST,2132S), PGC1 α (Novus Bio, NBP1-04676), Mst1(BD Transduction, 611052), p-PST1 (CST,3681S), mTOR (CST,2972S), p-mTOR (S2448) (CST, 2971S), ULK1 (Sigma-Aldrich, A7481), p-ULK1 (S555)(CST, 5869S), CD36 (Novus Bio, NB400-144), Ubiquitin (CST, 3933S), Tfam (Abcam, ab131607), and NRF1(Abcam,ab55744).

Echocardiographic analysis

This method has been described previously¹³. Mice were anesthetized using 12 μ l/g body weight of 2.5% Avertin (Sigma-Aldrich), and echocardiography was performed using ultrasonography (Acuson Sequoia C256; Siemens Medical Solutions) . A 13-MHz linear ultrasound transducer was used¹³. Two-dimensional guided M-Mode measurements of LV internal diameter were obtained from at least three beats and then averaged. LV end-diastolic diameter (LVEDD),

interventricular septal wall thickness (IVSWT), and posterior wall thickness (PWT) were obtained at the time of the apparent maximal LV diastolic dimension, whereas LV end-systolic diameter (LVESD) was obtained at the time of the most anterior systolic excursion of the posterior wall. LV fractional shortening was calculated as follows: fractional shortening = $(LVEDD-LVESD)/LVEDD \times 100$. All the analyses were performed in a blinded manner with regard to the genotype of mice.

Hemodynamic analysis

Pressure-volume analysis was performed using the Millar PV system MPVS 300/400 (Millar Instruments, Houston, Texas). After anesthesia with pentobarbital (60-70 mg/kg), the right carotid artery was cannulated with a high-fidelity Mikro-Tip catheter transducer (1.0-F, Model PVR-1030, Millar Instruments). LV diastolic and systolic pressures and performance were measured as previously described¹⁴.

Statistical analysis

Statistical analyses were conducted using the SPSS 23.0 program or Graph Pad Prism 8.0 software. In brief, the minimum sample size needed to detect changes obtained through preliminary experiments will be calculated with Power and Sample Size Analysis (<http://biostat.mc.vanderbilt.edu/wiki/Main/PowerSampleSize>), using 80% power and 5% significance level. Data was examined by Shapiro-Wilk normality test to determine normality. All data exhibited a normal distribution. Data are expressed as mean \pm SEM for the indicated number of experiments or mice. The difference

in means between 2 groups and multiple groups was evaluated using unpaired Student *t* test and one-way ANOVA, followed by Bonferroni post hoc test. P values were two-sided and p values of <0.05 were considered statistically significant.

Online Table I.

Pressure-volume loop data of HFD fed mice with ND or HFD.

	ND n=6	HFD2M n=6	HFD3M n=6	HFD4M n=6
HR, bpm	433±55	431±31	435±30	441±36
ESPVR, mmHg/ml	23.62±2.86	22.03±5.67	24.55±4.21	23.55±4.06
EDPVR, mmHg/ml	0.056±0.004	0.108±0.006 ^{&}	0.112±0.008 [#]	0.109±0.005 [*]
Tau,ms	7.05±0.41	8.88±0.25 ^{&}	9.30±0.33 [#]	10.23±0.17 [*]
+dP/dt, mmHg/s	6550±365	6480±330	7140±405	6355±672
-dP/dt, mmHg/s	7080±488	7124±313	6965±376	6510±552
LVEDP	6.45±0.41	8.29±0.31 ^{&}	8.9±0.21 [#]	9.23±0.56 [*]

HR, heart rate; ESPVR, end systolic pressure-volume relationship; EDPVR, end diastolic pressure-volume relationship; LV, left ventricle; EDP, end-diastolic pressure. Data are mean ± SEM, [&]p<0.05 vs ND, [#] p<0.05 vs ND, ^{*} p<0.05 vs ND using one way ANOVA followed by Bonferroni's *post-hoc* test.

Online Table II.

Echocardiographic data of WT, *atg7* cKO mice with ND or HFD.

	WT+ND n=6	<i>atg7</i> cKO +ND n=6	WT+HFD n=6	<i>atg7</i> cKO +HFD n=6
HR, bpm	490±24	486±30	480±34	504±27
LVEDD, mm	3.25±0.12	3.4±0.14	3.56±0.23	4.21±0.24* [‡]
LVESD,mm	2.11±0.15	2.23±0.25	2.35±0.18	3.39±0.32* [‡]
LVEF,%	72.6±4.1	70.1±5.2	71.2±5.8	40.4±7.4* [‡]
LVFS,%	35.1±2.1	34.5±2.3	34.1±3.1	19.5±4.2* [‡]
IVSWT,mm	1.08±0.02	1.06±0.09	1.19±0.05 [#]	0.98±0.1*
PWT,mm	1.04±0.03	0.96±0.18	1.18±0.07 [#]	0.88±0.12*

HR, heart rate; LV, left ventricle; EDD, end-diastolic dimension; ESD, end-systolic dimension; EF, ejection fraction; IVSWT, interventricular septal wall thickness; PWT, posterior wall thickness. Data are mean ± SEM, [#] p<0.05 vs WT+ND, * p<0.05 vs WT+HFD, [‡] p<0.05 vs WT+ND using one way ANOVA followed by Bonferroni's *post-hoc* test.

Online Table III.

Pressure-volume loop data of WT, *atg7* cKO mice with ND or HFD.

	WT+ND n=6	<i>atg7</i> cKO+ND n=7	WT+HFD n=7	<i>atg7</i> cKO+HFD n=8
HR, bpm	433±28	434±31	423±24	400±45
ESPVR, mmHg/ml	25.13±2.45	26.22±2.97	24.86±2.46	15.93±1.76* [‡]
EDPVR, mmHg/ml	0.051±0.009	0.061±0.006	0.11±0.004 [#]	0.152±0.019* [‡]
Tau,ms	7.14±0.55	8.93±0.65	9.32±1.26 [#]	17.57±3.55* [‡]
+dP/dt, mmHg/s	6267±233	6189±264	6502±332	5464±288* [‡]
-dP/dt, mmHg/s	7029±499	6768±211	6954±332	5324±234* [‡]
LVEDP	6.31±0.34	6.51±0.48	9.5±0.66 [#]	11.04±0.28* [‡]

HR, heart rate; ESPVR, end systolic pressure-volume relationship; EDPVR, end diastolic pressure-volume relationship; LV, left ventricle; EDP, end-diastolic pressure. Data are mean ± SEM, [#] p<0.05 vs WT+ND, * p<0.05 vs WT+HFD, [‡] p<0.05 vs WT+ND using one way ANOVA followed by Bonferroni's *post-hoc* test.

Online Table IV.

Pressure-volume loop data of WT, Parkin KO mice with ND or HFD.

	WT+ND n=5	Parkin KO n=5	WT+HFD n=6	Parkin KO+HFD n=6
HR, bpm	439±32	409±21	412±29	399±21
ESPVR, mmHg/ml	24.35±2.31	26.34±2.55	25.41±2.34	25.45±1.24
EDPVR, mmHg/ml	0.05±0.005	0.058±0.009	0.124±0.005 [#]	0.176±0.018 ^{*‡}
Tau,ms	7.34±0.23	8.81±0.46	8.98±1.11 [#]	9.47±1.05 [‡]
+dP/dt, mmHg/s	6325±202	6654±501	7001±662	6884±412
-dP/dt, mmHg/s	7009±305	6908±248	6853±538	6785±398
LVEDP	6.8±0.64	7.51±0.22	8.7±0.33 [#]	9.04±0.98 [‡]

HR, heart rate; ESPVR, end systolic pressure-volume relationship; EDPVR, end diastolic pressure-volume relationship; LV, left ventricle; EDP, end-diastolic pressure. Data are mean ± SEM, [#] p<0.05 vs WT+ND, ^{*} p<0.05 vs WT+HFD, [‡] p<0.05 vs WT+ND using one way ANOVA followed by Bonferroni's *post-hoc* test.

Online Table V.

Echocardiographic data of WT, Parkin KO mice with ND or HFD.

	WT+ND n=6	Parkin KO+ND n=6	WT+HFD n=6	Parkin KO +HFD n=6
HR, bpm	458±35	467±37	439±45	488±37
LVEDD, mm	3.34±0.11	3.45±0.23	3.69±0.22	3.62±0.31
LVESD,mm	2.10±0.10	2.25±0.15	2.27±0.10	2.35±0.15
LVEF,%	73.4±2.1	71.4±4.08	69.9±4.4	66.8±4.5
LVFS,%	36.1±1.9	35.5±2.3	38.5±5.6	36.6±4.5
IVSWT,mm	1.01±0.02	1.02±0.03	1.09±0.02 [#]	1.28±0.05 ^{*‡}
PWT,mm	1.03±0.04	1.01±0.05	1.11±0.01 [#]	1.25±0.06 ^{*‡}

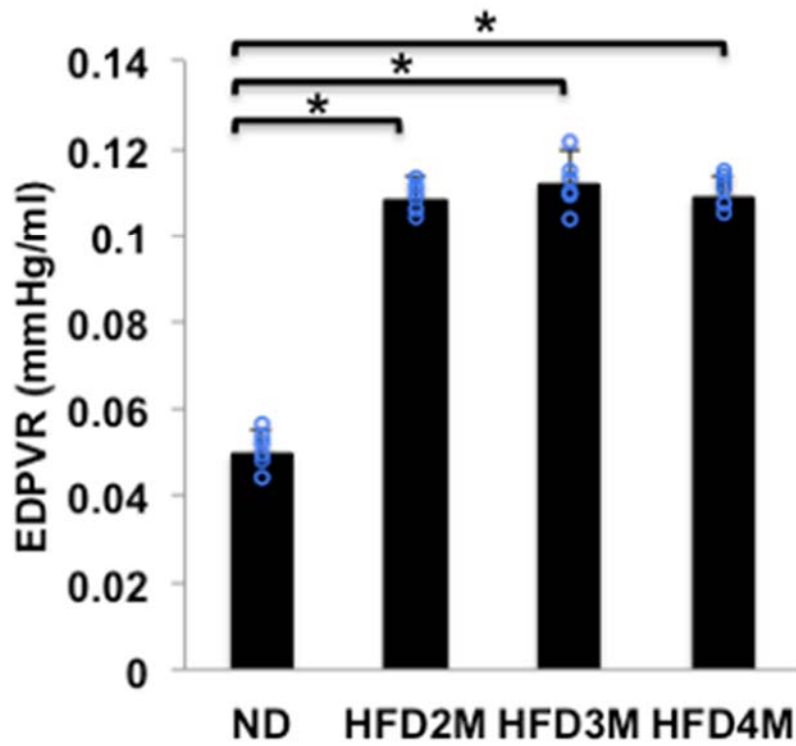
HR, heart rate; LV, left ventricle; EDD, end-diastolic dimension; ESD, end-systolic dimension; EF, ejection fraction; IVSWT, interventricular septal wall thickness; PWT, posterior wall thickness. Data are mean ± SEM, [#] p<0.05 vs WT+ND, ^{*} p<0.05 vs WT+HFD, [‡] p<0.05 vs WT+ND using one way ANOVA followed by Bonferroni's *post-hoc* test.

Online Table VI.

Pressure-volume loop data of TS, TB1 mice with ND or HFD.

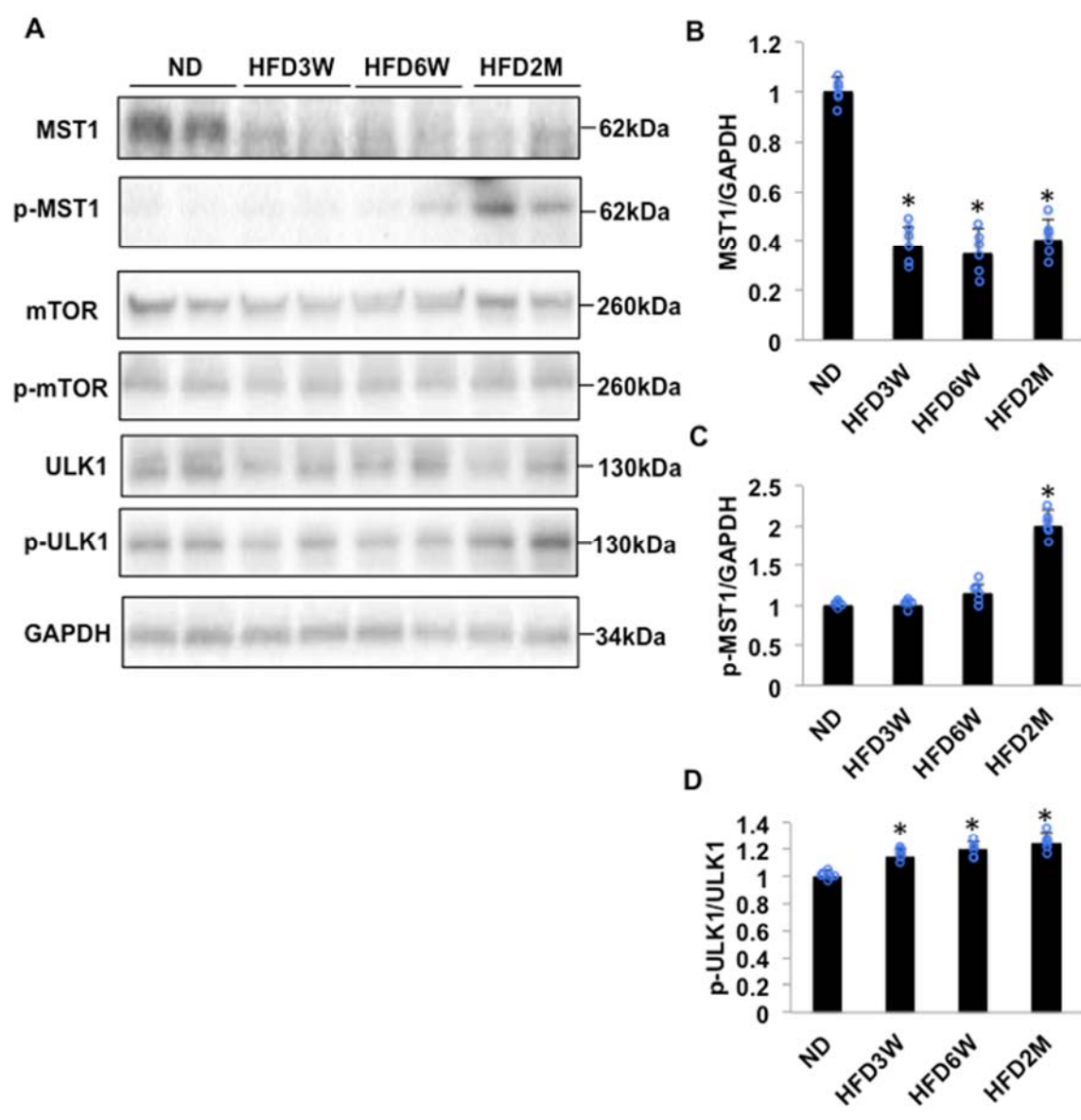
	TS+ND n=4	TB1+ND n=3	TS+HFD n=5	TB1+HFD n=5
HR, bpm	430±22	441±30	425±36	436±26
ESPVR, mmHg/ml	24.32±3.09	17.54±8.46	27.90±7.68	22.45±8.66
EDPVR, mmHg/ml	0.058±0.005	0.054±0.009	0.110±0.009 [#]	0.078±0.015 [*]
Tau,ms	7.09±0.45	8.01±0.34	9.44±0.42 [#]	7.57±0.86
+dP/dt, mmHg/s	6565±358	6425±378	7152±421	6376±698
-dP/dt, mmHg/s	7091±476	7159±343	6993±419	6539±588
LVEDP	6.55±0.45	7.09±0.34	8.9±0.81 [#]	6.03±0.89

HR, heart rate; ESPVR, end systolic pressure-volume relationship; EDPVR, end diastolic pressure-volume relationship; LV, left ventricle; EDP, end-diastolic pressure. Data are mean ± SEM, [#] p<0.05 vs WT+ND, ^{*} p<0.05 vs WT+HFD using one way ANOVA followed by Bonferroni's *post-hoc* test.



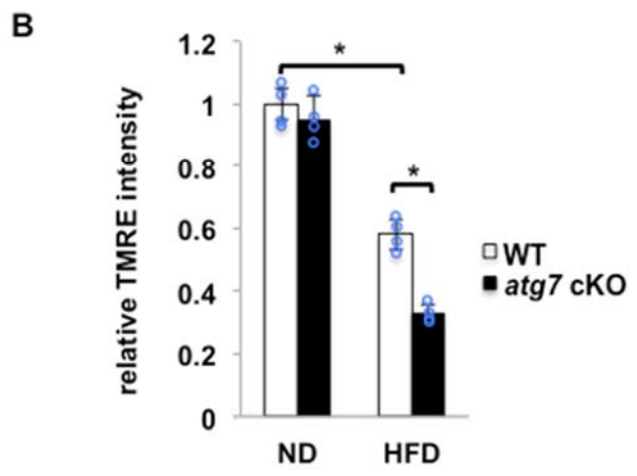
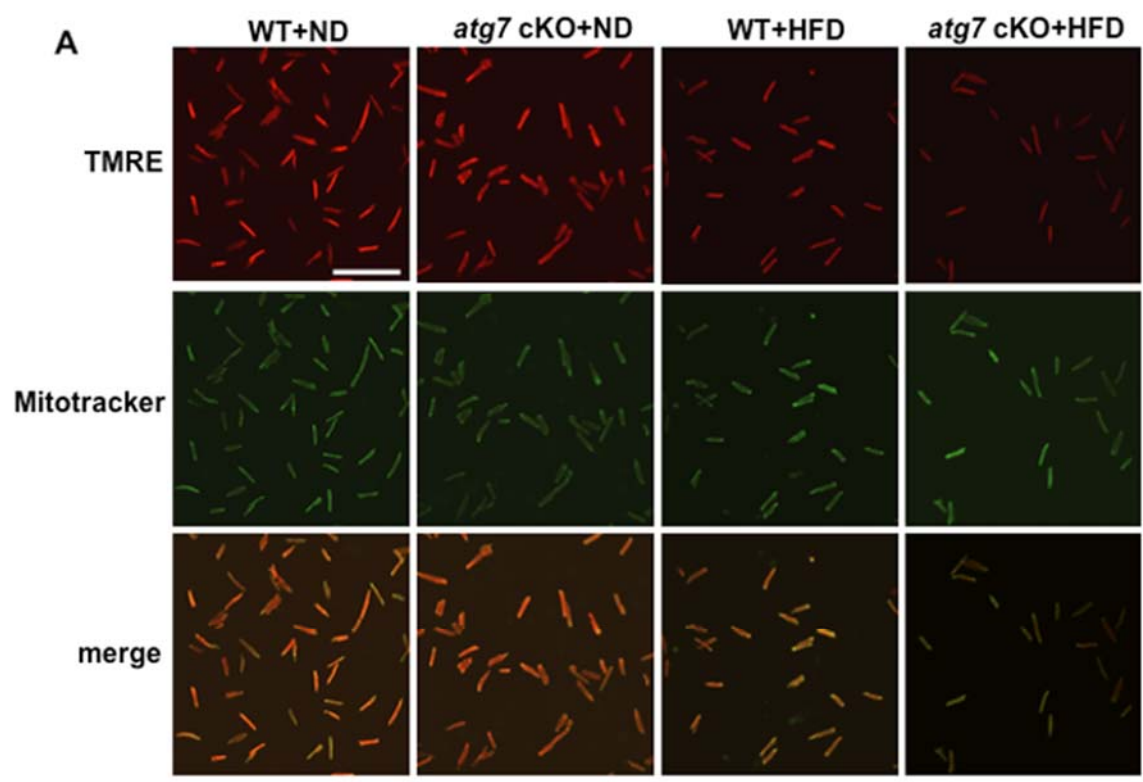
Online Figure I.

EDPVR evaluated by PV-Loop analysis showed that cardiac diastolic dysfunction had developed after two months of HFD feeding. N=5-6 in each group. Values are means \pm S.E. *, $p < 0.05$ using unpaired Student *t* test.

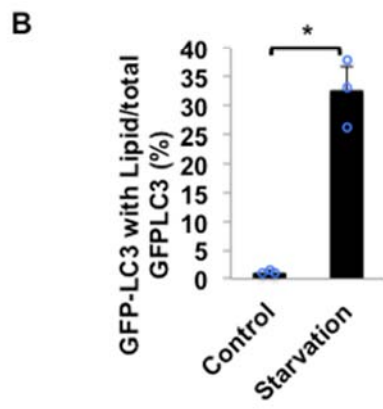
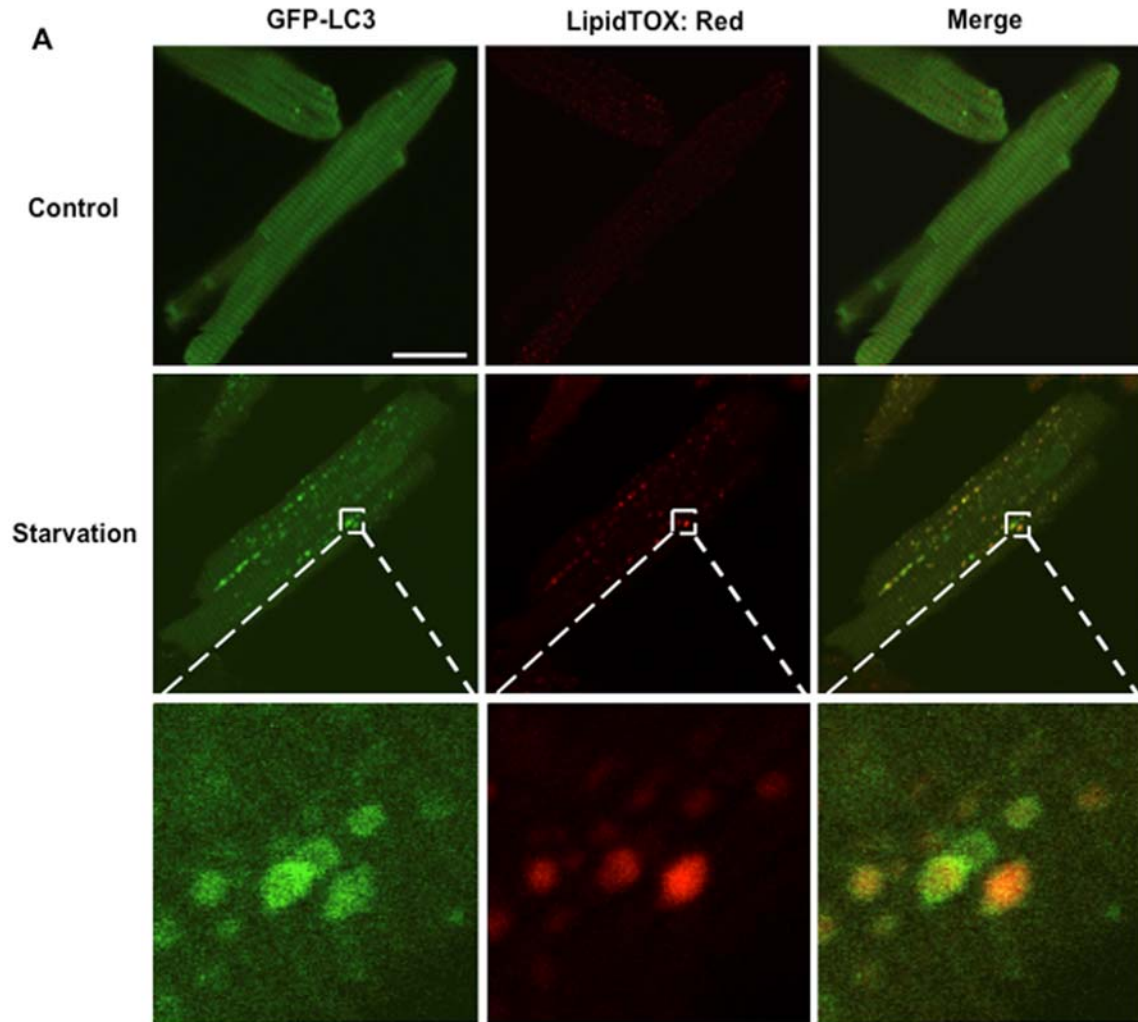


Online Figure II.

(A-D) Representative immunoblots and quantitative analyses of whole-cell heart homogenates for upstream pathways of autophagy at different time points following HFD consumption in mice. N=6 in each group. Values are means \pm S.E. *, $p < 0.05$ using unpaired Student *t* test.

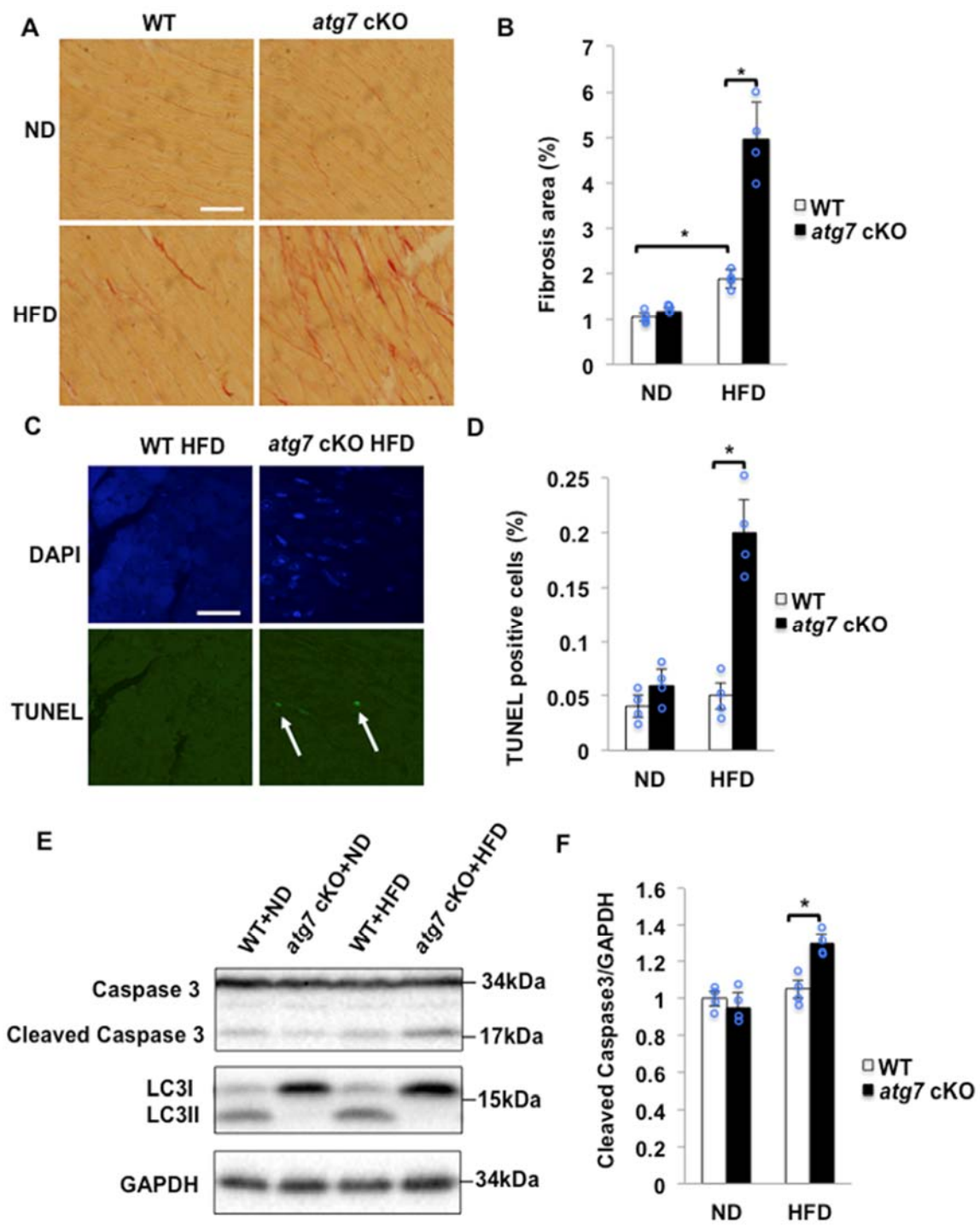


Online Figure III. (A,B) WT and *atg7* cKO mice were fed with either ND or HFD for 2 months. CMs were freshly isolated and subjected to TMRE staining. Representative fluorescent images and quantitative analysis of TMRE staining. Mitochondrial membrane potential was decreased in *atg7* cKO mice. N=4 in each group. Values are means \pm S.E. *, $p < 0.05$ using unpaired Student *t* test. Scale bar = 500 μ m.



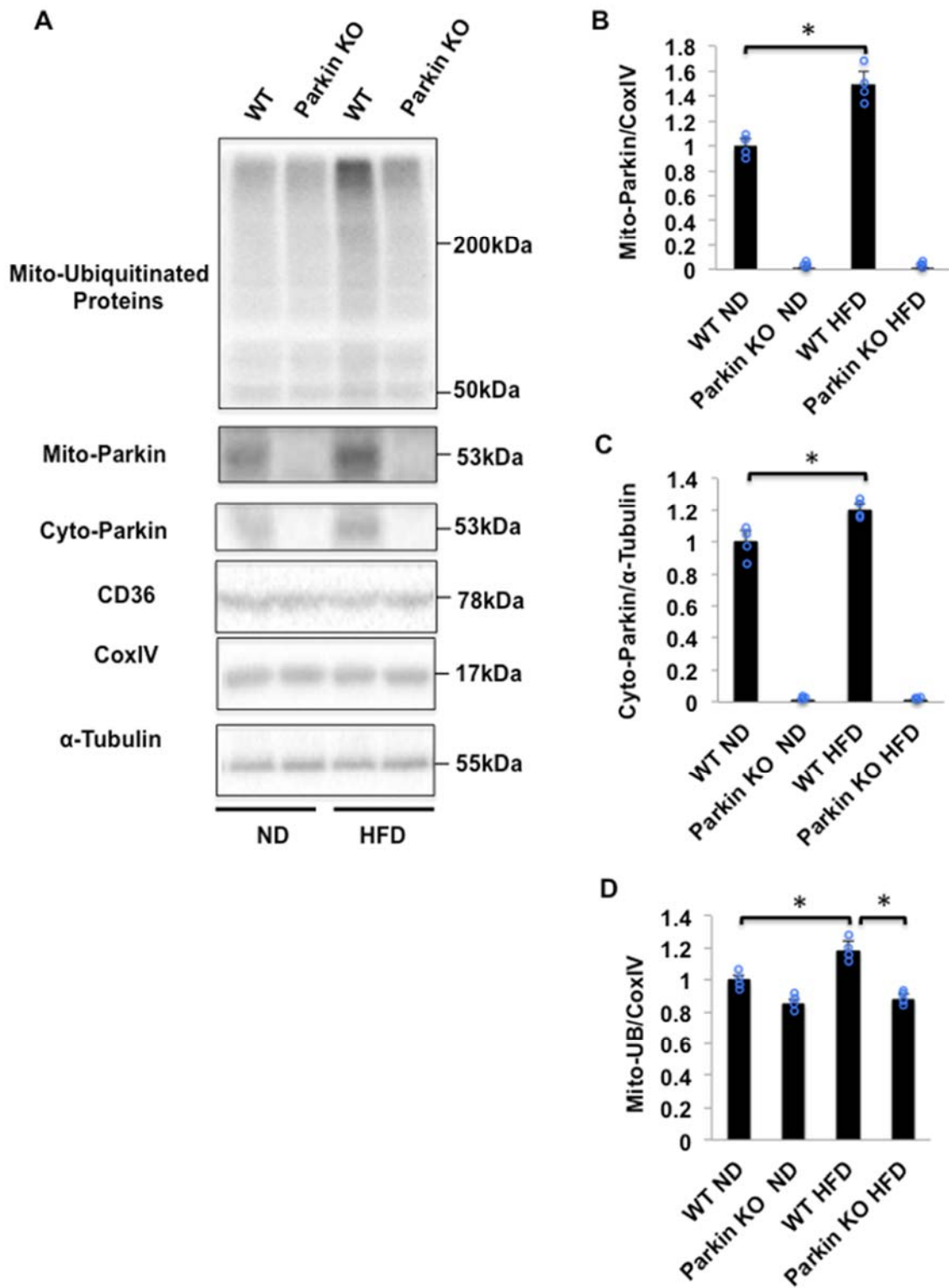
Online Figure IV.

Co-localization of GFP-LC3 with lipids in CMs freshly isolated from mice with starvation condition. (A, B) Representative fluorescent images and quantitative analyses of adult CMs isolated from cardiac Tg-GFP-LC3 mice subjected to either control or starvation. CMs were incubated with lipidTOX red. GFP-LC3 rings with lipid were observed during starvation 48 hours. N=3 in each group. Values are means \pm S.E. *, $p < 0.05$ using unpaired Student *t* test. Scale bar = 50 μm .



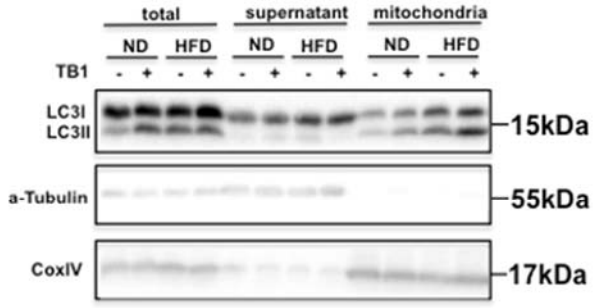
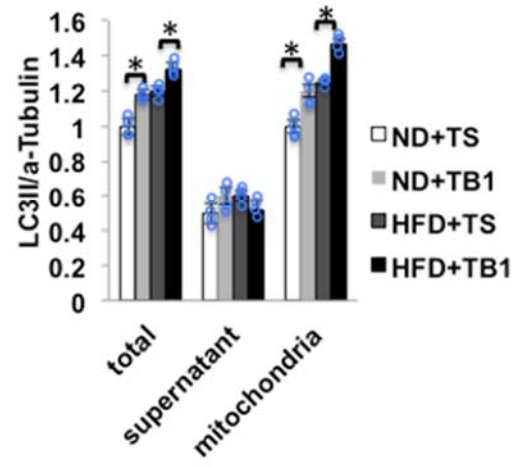
Online Figure V.

WT and *atg7* cKO mice were fed to either ND or HFD feeding for 2 months. (A) Myocardial sections were subjected to Picrosirius red (PSR) staining for the evaluation of cardiac fibrosis. Fibrosis increased more in *atg7* cKO mice than in WT mice in response to HFD feeding. Scale bar = 100 μ m. (B) Quantification of the fibrosis area in the heart. N=4 in each group. Values are means \pm S.E. *, $p < 0.05$ using one way ANOVA followed by Bonferroni's *post-hoc* test. (C-F) Cell death was increased in *atg7* cKO mice fed with HFD. (C,D) Representative TUNEL staining and quantitative analyses of apoptosis. N=4 in each group. Values are means \pm S.E. *, $p < 0.05$ using one way ANOVA followed by Bonferroni's *post-hoc* test. Scale bar = 100 μ m. (E,F) Immunoblot analyses and quantification of cleaved caspase 3 and GAPDH. N=4 in each group. Values are means \pm S.E. *, $p < 0.05$ using one way ANOVA followed by Bonferroni's *post-hoc* test.



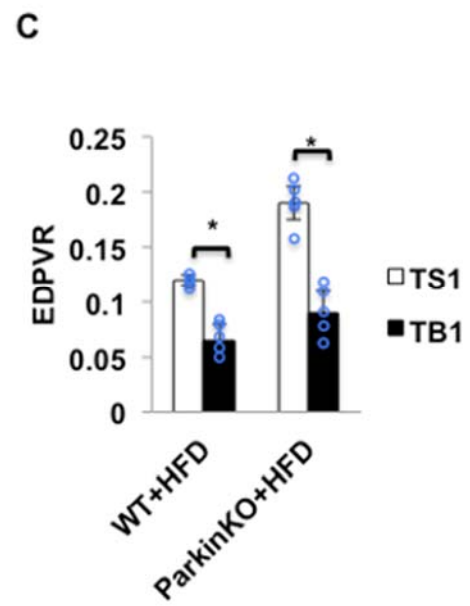
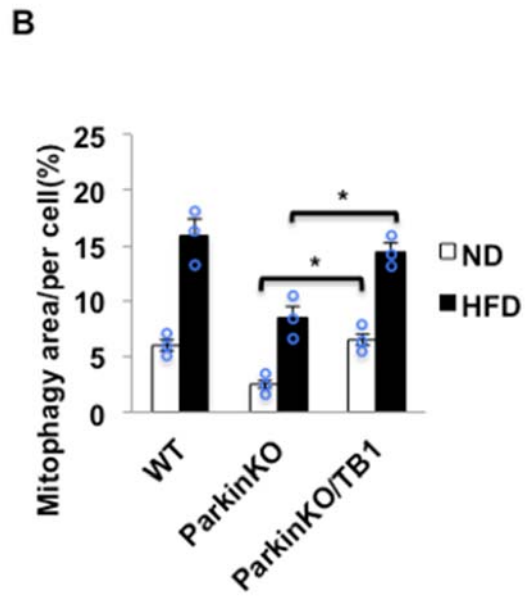
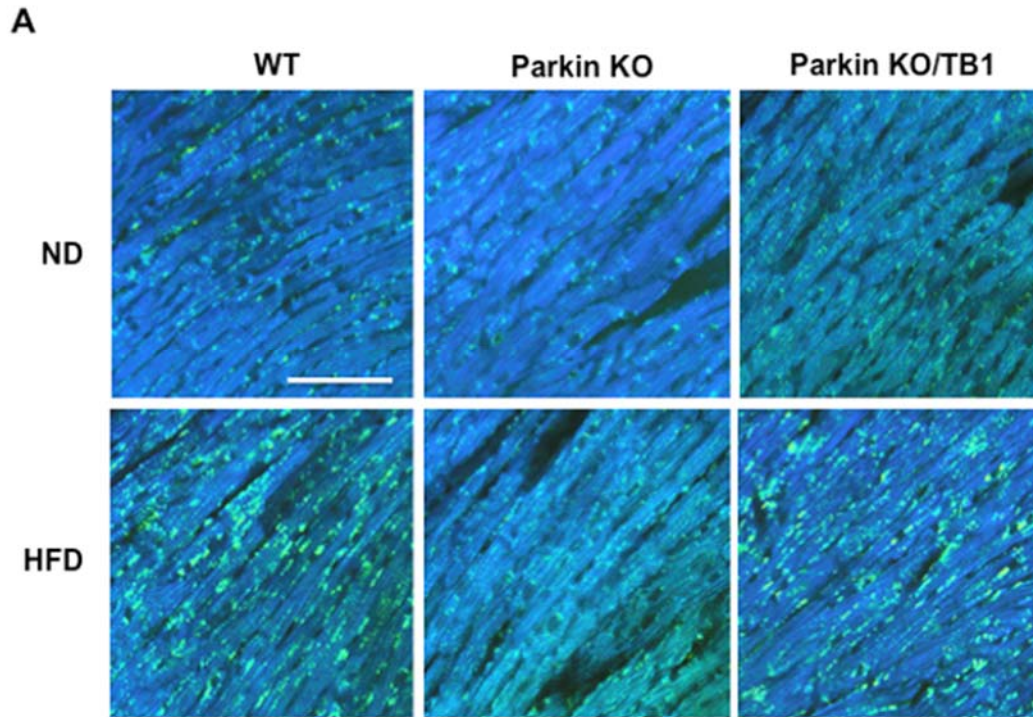
Online Figure VI.

(A-D) Representative immunoblots and quantitative analyses of whole-cell heart homogenates and mitochondrial fractions examining Parkin and ubiquitinated protein levels. N=4 in each group. Values are means \pm S.E. *, $p < 0.05$ using unpaired Student *t* test.

A**B**

Online Figure VII.

(A-B) Representative immunoblots and quantitative analyses of whole-cell heart homogenates and mitochondrial fractions examining LC3II level. N=4 in each group. Values are means \pm S.E. *, $p < 0.05$ using unpaired Student *t* test.



Online Figure VIII.

HFD-induced cardiac dysfunction in Parkin KO mice was attenuated by TB1.

(A,B) Mitophagy was restored in Parkin KO mice following injection of TB1.

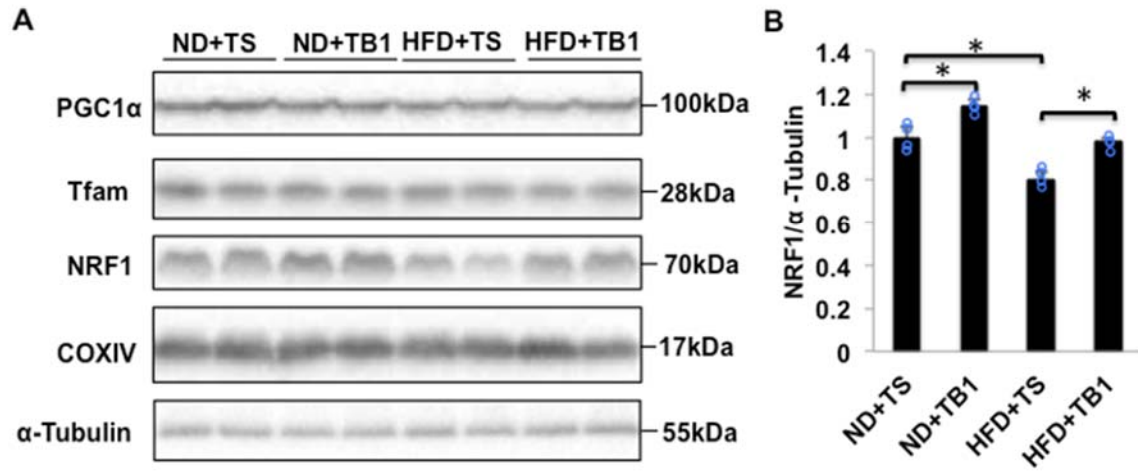
Parkin KO mice crossed with Tg-Mito-Keima mice were fed ND or HFD for 2 months. Mice were injected intraperitoneally with TS or TB1 at 20 mg/kg daily for 2 weeks, beginning after 8 weeks of HFD feeding. Areas with high ratios

(561/457) of Mito-Keima signal, indicating mitophagy, are shown. Representative fluorescent images and quantitative analysis of mitophagy. Scale bar = 50 μ m.

N=3 in each group. Values are means \pm S.E. *, $p < 0.05$ using unpaired Student *t*

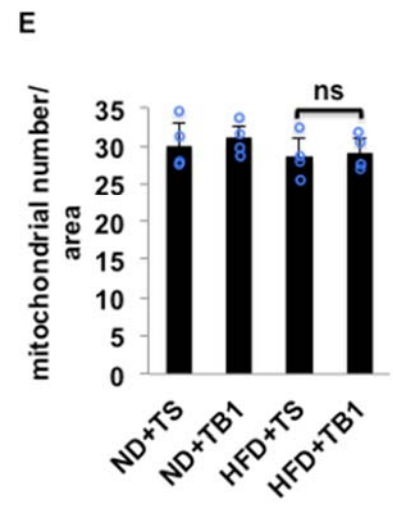
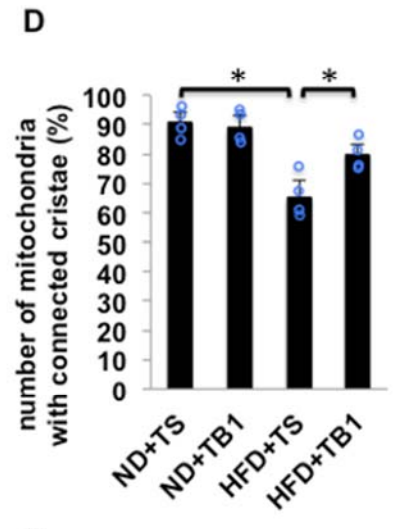
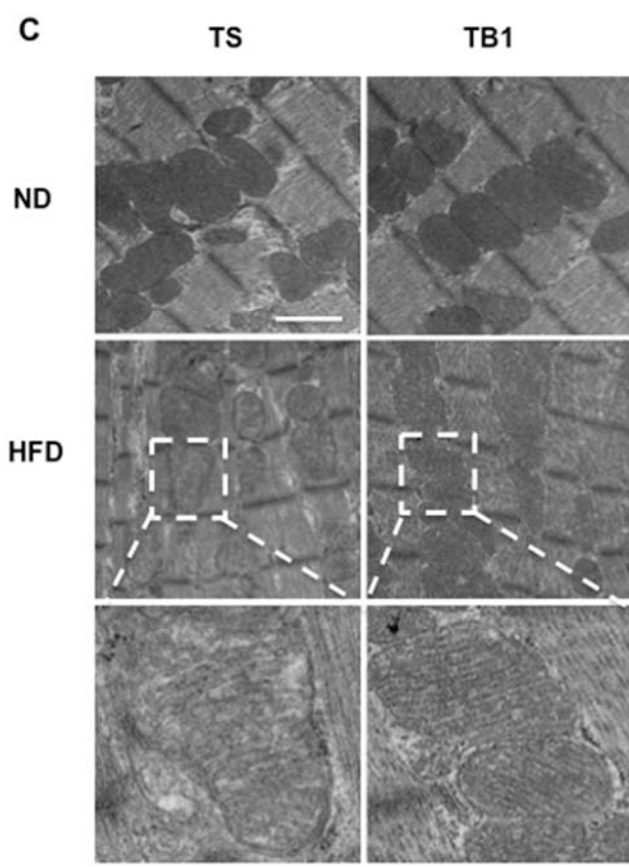
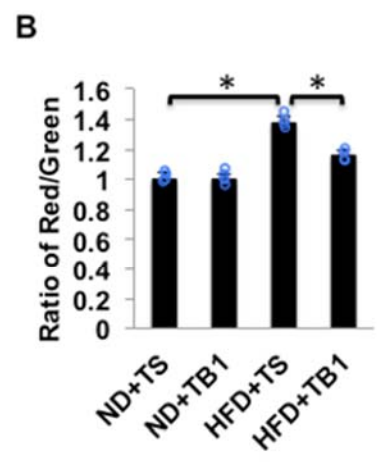
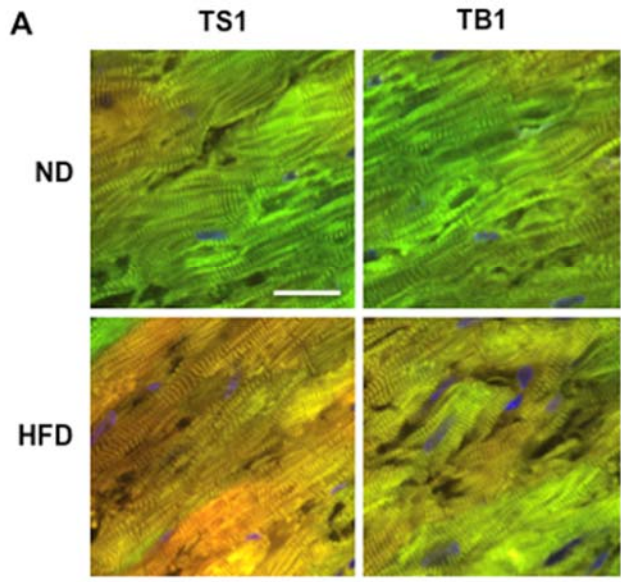
test. (C) EDPVR evaluated by PV-Loop analysis showed that HFD-induced cardiac diastolic dysfunction was attenuated by injection of TB1 compared with

TS. N=3-5 in each group. Values are means \pm S.E. *, $p < 0.05$ using unpaired Student *t* test.



Online Figure IX.

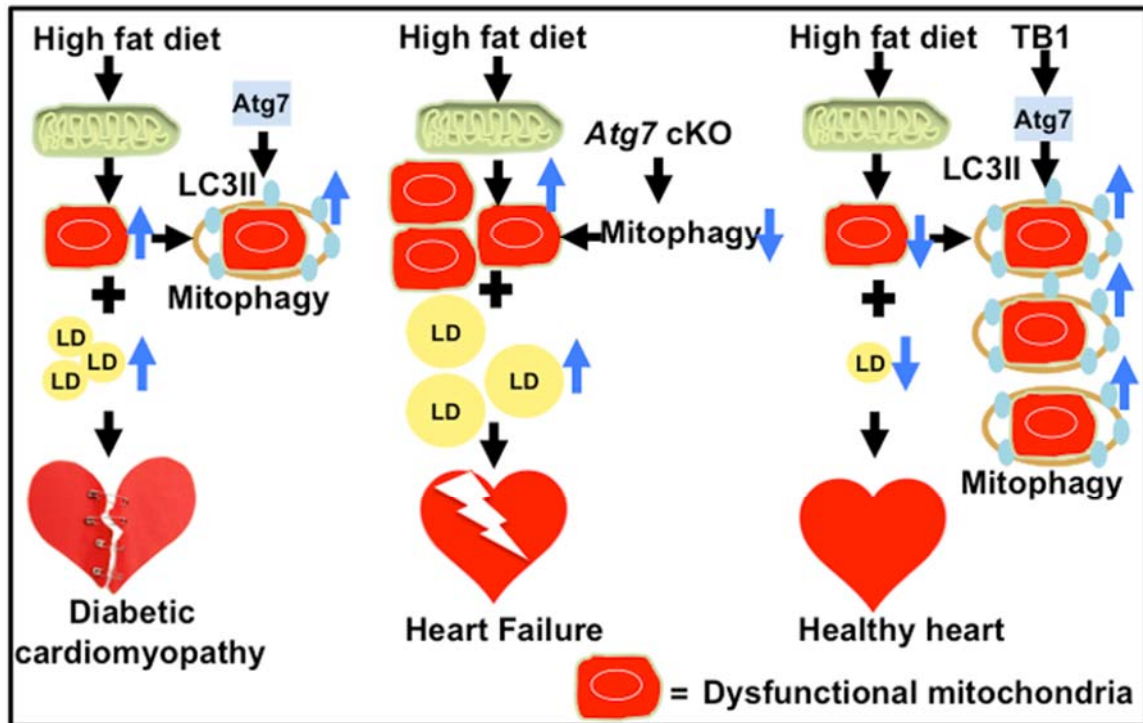
(A-B) Representative immunoblots and quantitative analysis of whole-cell heart homogenates examining transcription factors involved in mitochondrial biogenesis. N=4 in each group. Values are means \pm S.E. *, $p < 0.05$ using unpaired Student *t* test.



Online Figure X.

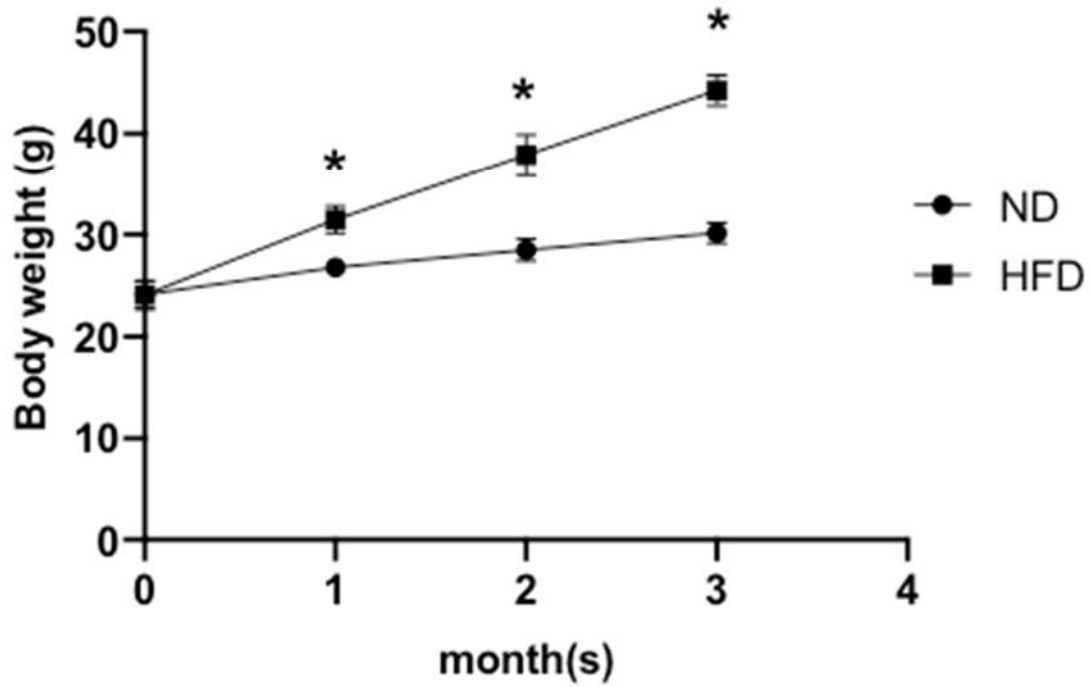
(A-B) Representative fluorescent images and quantitative analyses of Mitotimer in heart tissue from Tg-Mitotimer mice. Mitotimer mice were fed ND or HFD for 3 months. Mice were injected intraperitoneally with TS or TB1 at 20 mg/kg daily for 2 weeks, beginning after 10 weeks of HFD feeding. Scale bar = 50 μ m. N=4 in each group. Values are means \pm S.E. *, $p < 0.05$ using unpaired Student *t* test.

(C-D) Representative EM images and quantitative analyses of mouse hearts. N=4 in each group. Values are means \pm S.E. *, $p < 0.05$ using unpaired Student *t* test. Scale bar = 500 nm. (E) Quantitative analyses of mitochondrial number from EM images of mouse hearts. N=4 in each group. “ns” indicates not significant ($p > 0.05$ using unpaired Student *t* test).



Online Figure XI.

A scheme for the role of mitophagy in diabetic cardiomyopathy. Mitophagy was activated during HFD consumption through Atg7-dependent autophagy. Absence of Atg7 impairs mitophagy, decreases mitochondrial function, increases lipid accumulation, and exacerbates cardiac dysfunction during HFD feeding. Injection of TB1 activates mitophagy, attenuates mitochondrial dysfunction, decreases lipid accumulation, and protects against cardiac diastolic dysfunction during HFD feeding.



Online Figure XII.

Graph showing body weight gain at different time points in mice fed a ND or a HFD. N=30 in each group. Values are mean \pm S.E. *, $p < 0.05$ using unpaired Student *t* test.

References:

1. Komatsu M, Waguri S, Ueno T, Iwata J, Murata S, Tanida I, Ezaki J, Mizushima N, Ohsumi Y, Uchiyama Y, Kominami E, Tanaka K and Chiba T. Impairment of starvation-induced and constitutive autophagy in Atg7-deficient mice. *The Journal of cell biology*. 2005;169:425-34.
2. Hariharan N, Zhai P and Sadoshima J. Oxidative stress stimulates autophagic flux during ischemia/reperfusion. *Antioxidants & redox signaling*. 2011;14:2179-90.
3. Ackers-Johnson M, Li PY, Holmes AP, O'Brien SM, Pavlovic D and Foo RS. A Simplified, Langendorff-Free Method for Concomitant Isolation of Viable Cardiac Myocytes and Nonmyocytes From the Adult Mouse Heart. *Circulation research*. 2016;119:909-20.
4. Katayama H, Kogure T, Mizushima N, Yoshimori T and Miyawaki A. A sensitive and quantitative technique for detecting autophagic events based on lysosomal delivery. *Chemistry & biology*. 2011;18:1042-52.
5. Ikeda Y, Shirakabe A, Maejima Y, Zhai P, Sciarretta S, Toli J, Nomura M, Mihara K, Egashira K, Ohishi M, Abdellatif M and Sadoshima J. Endogenous Drp1 mediates mitochondrial autophagy and protects the heart against energy stress. *Circulation research*. 2015;116:264-78.
6. Oka S, Alcendor R, Zhai P, Park JY, Shao D, Cho J, Yamamoto T, Tian B and Sadoshima J. PPARalpha-Sirt1 complex mediates cardiac hypertrophy and failure through suppression of the ERR transcriptional pathway. *Cell metabolism*. 2011;14:598-611.
7. Watanabe K, Fujii H, Takahashi T, Kodama M, Aizawa Y, Ohta Y, Ono T, Hasegawa G, Naito M, Nakajima T, Kamijo Y, Gonzalez FJ and Aoyama T. Constitutive regulation of cardiac fatty acid metabolism through peroxisome proliferator-activated receptor alpha associated with age-dependent cardiac toxicity. *The Journal of biological chemistry*. 2000;275:22293-9.
8. Shirakabe A, Zhai P, Ikeda Y, Saito T, Maejima Y, Hsu CP, Nomura M, Egashira K, Levine B and Sadoshima J. Drp1-Dependent Mitochondrial Autophagy Plays a Protective Role Against Pressure Overload-Induced Mitochondrial Dysfunction and Heart Failure. *Circulation*. 2016;133:1249-63.
9. Shoji-Kawata S, Sumpter R, Leveno M, Campbell GR, Zou Z, Kinch L, Wilkins AD, Sun Q, Pallauf K, MacDuff D, Huerta C, Virgin HW, Helms JB, Eerland R, Tooze SA, Xavier R, Lenschow DJ, Yamamoto A, King D, Lichtarge O, Grishin NV, Spector SA, Kaloyanova DV and Levine B. Identification of a candidate therapeutic autophagy-inducing peptide. *Nature*. 2013;494:201-6.
10. Iwai-Kanai E, Yuan H, Huang C, Sayen MR, Perry-Garza CN, Kim L and Gottlieb RA. A method to measure cardiac autophagic flux in vivo. *Autophagy*. 2008;4:322-9.
11. Matsui Y, Takagi H, Qu X, Abdellatif M, Sakoda H, Asano T, Levine B and Sadoshima J. Distinct roles of autophagy in the heart during ischemia and

reperfusion: roles of AMP-activated protein kinase and Beclin 1 in mediating autophagy. *Circulation research*. 2007;100:914-22.

12. Hariharan N, Maejima Y, Nakae J, Paik J, Depinho RA and Sadoshima J. Deacetylation of FoxO by Sirt1 Plays an Essential Role in Mediating Starvation-Induced Autophagy in Cardiac Myocytes. *Circulation research*. 2010;107:1470-82.

13. Ikeda S, Mizushima W, Sciarretta S, Abdellatif M, Zhai P, Mukai R, Fefelova N, Oka SI, Nakamura M, Del Re DP, Farrance I, Park JY, Tian B, Xie LH, Kumar M, Hsu CP, Sadayappan S, Shimokawa H, Lim DS and Sadoshima J. Hippo Deficiency Leads to Cardiac Dysfunction Accompanied by Cardiomyocyte Dedifferentiation During Pressure Overload. *Circulation research*. 2019;124:292-305.

14. Pacher P, Nagayama T, Mukhopadhyay P, Batkai S and Kass DA. Measurement of cardiac function using pressure-volume conductance catheter technique in mice and rats. *Nature protocols*. 2008;3:1422-34.